Multi-Satellite Precipitation Products for Meteorological Drought Assessment and Forecasting in Bundelkhand region of Central India

Varsha Pandey, Prashant K Srivastava, R K Mall, Francisco Munoz-Arriola & Dawei Han

Multi-Satellite Precipitation Products for Meteorological Drought Assessment and Forecasting in Bundelkhand region of Central India

Varsha Pandey[a], Prashant K Srivastava[a,b*], R K Mall[b], Francisco Munoz-Arriola[c,d], Dawei Han[e]

[a]Remote Sensing Laboratory, Institute of Environment and Sustainable Development, Banaras Hindu University, Varanasi, Uttar Pradesh 221005, India

[b]DST-Mahamana Center for Excellence in Climate Change Research, Institute of Environment and Sustainable Development, Banaras Hindu University, Varanasi, Uttar Pradesh 221005, India

[c]School of Natural Resources, University of Nebraska-Lincoln, USA

[d]Department of Biological Systems Engineering, University of Nebraska-Lincoln, USA

[e]Department of Civil Engineering, University of Bristol, UK

*Corresponding author E-mail: prashant.just@gmail.com; prashant.iesd@bhu.ac.in

Abstract

In this study, a comparative analysis of three satellite precipitation products including Tropical Rainfall Measuring Mission (TRMM-3B43 V7), Precipitation Estimation from Remotely Sensed Information using Artificial Neural Networks-Climate Data Record (PERSIANN-CDR), and Climate Hazards Group InfraRed Precipitation with Station (CHIRPS V2) with ground-measured Indian Meteorological Department (IMD) precipitation data were performed to estimate the meteorological drought in the Bundelkhand region of Central India. The high-resolution CHIRPS data showed the closest agreement with the IMD precipitation and well captured the drought characteristics. The Standardized Precipitation Index (SPI) identified seven major droughts

events during the period of 1981 to 2016. Appropriate calibration and validation were performed for drought forecasting using the Auto-Regressive Integrated Moving Average (ARIMA) model. The forecasting result showed a reasonably good agreement with the observed datasets with the one-month lead time. The outcomes of this study have policy level implications for drought monitoring and preparedness in this region.

Keywords: SPI; Meteorological drought; Precipitation; ARIMA model; Forecasting

1. Introduction

Most of the Indian states are severely affected by recurrent and prolonged drought events that lead to high water scarcity and adversely affect the crop yields, livestock, allied sectors, and thereby socioeconomic condition, along with natural vegetation, groundwater recharge, etc. (Glantz 1994, Bandyopadhyay *et al.* 2020). Drought is characterized as a stochastic phenomenon with indistinct onset and ends, undefined structure, and its slower impact that accumulated over a considerable period (Yaduvanshi *et al.* 2015). Considering its complexity, nature, and impact, drought has been grouped into four types: meteorological, agricultural, hydrological, and socioeconomic (Wilhite and Glantz 1985, Wilhite 2000). The meteorological drought is initiated with a significant deficit of precipitation from long term climatology and reduces soil moisture, groundwater, streamflow, and other water storages.

In recent years, drought events become more recurrent and severe due to global climate alteration (Jentsch and Beierkuhnlein 2008). Numerous studies have indicated that precipitation is the precursor of onset and persistence of meteorological and other drought types (Heim Jr 2002, Hao and Singh 2015). Therefore, reliable measurement of precipitation at different temporal and spatial scales is important for drought hazard assessment. Although the rain gauge

2

observation provides accurate and long-term records, there are several limitations such as coarse spatial coverage due to sparse or nonhomogeneous networks, discontinuity in data records, high maintenance cost, etc. which constraint the accurate drought assessment and monitoring especially in developing countries. On the other hand, the satellite remote sensing-based precipitation products offer a powerful alternative data having much higher spatial resolution that are continuous spatially and temporally (Pandey *et al.* 2019, Pandey and Srivastava 2019a). These datasets provide global monitoring of precipitation and widely used for different hydrological and climatic applications as they fill data voids over inaccessible areas where conventional rain gauge and ground radar measurements are limited or unavailable. The accuracy of different satellite-based precipitation products varies greatly depending on the working principle, sensor type, range of electromagnetic spectra used in generating the products such as microwave, Infrared, and Visible or combined range, numbers of integrated observational networks, data processing algorithms and resampling techniques. Several attempts were made on comparative analysis of these satellite precipitation products by available ground observed data. Stisen and Sandholt (2010) evaluated the performance of five satellite-based precipitation products through the input specific calibration capability of the distributed hydrological models over the Senegal River basin in West Africa. The statistical evaluation of daily precipitation rates of high-resolution PERSIANN, TMPA-3B42V7, and TMPA-3B42RT was carried out by Moazami *et al.* (2013). Sharifi *et al.* (2016) compared the multi-satellite retrieval for GPM, TRMM, TMPA-3B42, and the Era-Interim product from the European Centre for Medium Range Weather Forecasts (ECMWF) precipitation products in different climatic and topographic regions in Iran. Recently, Dandridge *et al.* (2019) statistically evaluated the TMPA 3B42 v.7 and CHIRPS data at various temporal scales in the Lower Mekong River basin (LMRB) in Southeast

Asia for drought assessment. The satellite precipitation data evaluations were mostly carried out at the global scale (Beck *et al.* 2017, Zhao and Ma 2019), continental scale (Xie *et al.* 2007, Peña-Arancibia *et al.* 2013, Awange *et al.* 2016, Kimani *et al.* 2017) country level (Shen *et al.* 2010, Miao *et al.* 2015, Alijanian *et al.* 2017, Prakash 2019), and regional scale (Hirpa *et al.* 2010, Gao and Liu 2012, Jiang *et al.* 2012). However, a similar assessment at the local scale is inadequate, leads to highly uncertain output while satellite-based precipitation data products are used.

Various indicators are used to identify drought conditions by investigating the deviation of climatic variables from the long-term average value. The Standardized Precipitation Index (SPI) is a compliant index that popularly used for meteorological drought assessment and also recommended by the World Meteorological Organization (WMO). SPI is extensively used to assess various aspects of drought events including frequency (McKee *et al.* 1993), intensity (Naresh Kumar *et al.* 2009), spatio-temporal distribution (Umran Komuscu 1999, SIRDAŞ and Sen 2003, Kalisa *et al.* 2020), and forecasting (Mishra and Desai 2005). SPI is also preferred because of its versatility, flexibility in time scale, and especially its dependency on precipitation data only. The modeling and forecasting of drought conditions using the time-series analysis rely on the past and present observations, which are highly challenging due to the stochastic nature of drought events. However, such projections have high usefulness in prior preparedness via advance mitigation and management strategies, most importantly in the field agriculture and water resource management activities (Gupta *et al.* 2020). Several studies have utilized the simplistic but efficient time series analysis approaches for drought projection, such as Autoregressive Integrated Moving Average (ARIMA) models, neural network, exponential smoothening, etc. using SPI (Mishra and Desai 2006, Morid *et al.* 2007, Han *et al.* 2012, Maca

and Pech 2016). The ARIMA model uses a statistical approach to predict reliable drought trend and have several advantages over other techniques such as fixed structure, specificity for time series, easiness, computationally inexpensive, dependency over skill and experience of the data analyst, use of backward observations, etc. (Mishra and Desai 2005, Yurekli *et al.* 2005, Fernández *et al.* 2009). ARIMA time series model is a structured empirical technique for forecasting and analyzing the stochastic nature of drought. When the time series data is stationary and linear, the Auto Regressive (AR) or Moving Average (MA) or mixed Auto Regressive Moving Average (ARMA) models are applied. However, when time series data is non-stationary and non-linear, the differencing is applied before the application of Auto Regressive Integrated Moving Average (ARIMA) (Hamilton 1994, Contreras *et al.* 2003).

This study aims to identify the most accurate satellite-based precipitation product at a local scale, to assess and forecast the drought condition in the study site to assist water resource managers for improved management activities and policies. The specific objectives of this study are 1) to evaluate the reliability of different satellite-based precipitation products for meteorological drought assessment at a local scale, 2) to assess meteorological drought using Standardized Precipitation Index (SPI) in a drought-prone region (Bundelkhand region of Uttar Pradesh, India) for 36 years (1981-2016), and 3) to forecast drought condition (SPI) employing ARIMA model. It should be emphasized that the high-resolution CHIRPS data has been used in this study, which was not used previously in any Indian site for drought assessment and forecasting.

2. Site Description

The study site is the Bundelkhand region of Uttar Pradesh, India; where the socio-economic condition is primarily dependent on agriculture and allied sectors. The region comprises of seven districts and stretches between the latitude 24°18' and 26°45' N and the longitude 78°16' and 81°56' E, covering an area of around 29485.34 km^2 (**Figure** 1). The altitude in the study area ranges between 58 m to 619 m above mean sea level, with the slope from north to south. Bundelkhand region has a semi-arid climatic condition, lies in the dry Vindhyan plateau, and characterized by four distinctive seasons i.e., winter, summer, monsoon, and post-monsoon (Gupta *et al.* 2014). This region is a rain-fed area, where precipitation is very erratic, uncertain and has a poor supply in terms of late-onset of monsoon, early withdrawal of precipitation. The annual average rainfall ranges from 665 mm to 1035 mm, concentrated mostly in the monsoon season (June-September: JJAS) (https://data.gov.in). Bundelkhand region is plagued by underdevelopment and poverty, experiences recurrent drought events, which aggravates the food insecurity in the region. The water scarcity due to recurrent drought conditions with nutrient deficit soil and low productivity makes agriculture under-invested, risky, and vulnerable. The adverse conditions increased the demand for drought monitoring and effective mitigation strategies in this region.
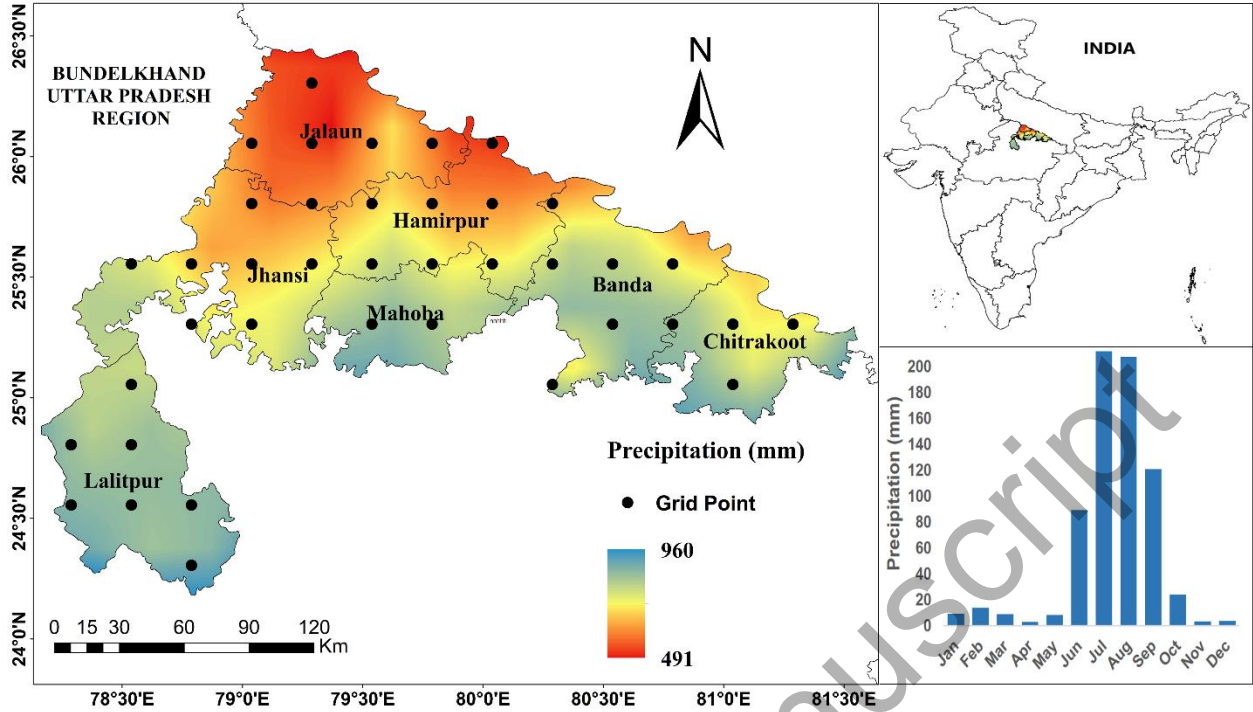
Figure 1. IMD derived mean annual precipitation map of the study area for the period of 1998 to 2016 overlaid by the IMD grid center points. The inset displays the monthly precipitation climatology of the Bundelkhand UP region.

3. Data and Methods

3.1. The Observed Precipitation Data

For validating satellite precipitation data products, the observed precipitation records were accessed from the archives of the National Data Center, India Meteorological Department (IMD) that is used optimally for various meteorological applications. The gridded IMD precipitation product uses around 6955 rain gauge stations across India, whereas at daily scale the number of reported gauges may vary. The Inverse Distance Weighted (IDW) interpolation technique is employed to create continuous or gridded precipitation data at 0.25° spatial resolution (Pai *et al.* 2014). Based on the availability of satellite precipitation data products, the IMD precipitation data was accessed for the period of 1998-2016, which was used as a reference for comparing

satellite precipitation data products and the precipitation-data derived SPI for drought monitoring. The overall methodology used in this study is shown in **Figure 2**.
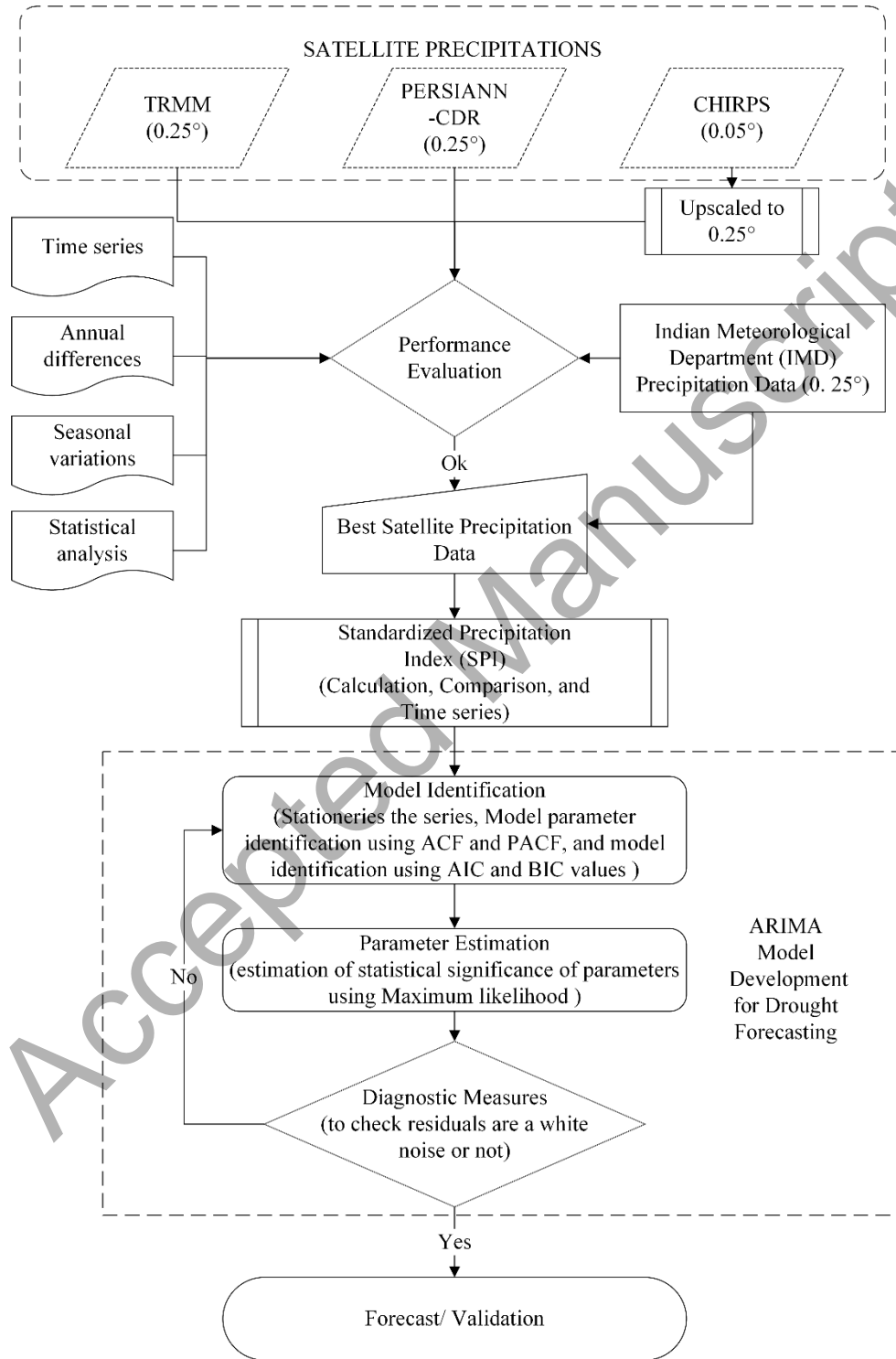

Figure 2. The workflow of the methodology

3.2. Satellite Precipitation Datasets

Three multi-satellite precipitation products were assessed namely, TRMM, CHIRPS, and PERSIANN-CDR from 1998 to 2016, based on the common period of data availability (**Table 1**). The Tropical Rainfall Measuring Mission (TRMM) Multisatellite Precipitation Analysis (TMPA) 3B43 version 7 products are widely used in monitoring and studying tropical and subtropical precipitation measurements for various hydro-climatological applications such as drought assessment, flood prediction, and hydrological modeling. Recently, Chen et al. (2020) evaluated the TRMM 3B43 precipitation product and suggested its applicability for reliable drought monitoring over the Yangtze River basin. Fereidoon *et al.* (2019) used the TRMM products for calibrating the SWAT (Soil and Water Assessment Tool) hydrological model to simulate runoff for flood prediction in Iran. Fang et al. (2019) integrated the TRMM 3B42 and the Global Precipitation Measurement Integrated Multi-satellite Retrievals (GPM IMERG) data to estimate extreme precipitation events over China and observed the high potentiality of merged product to better represent the spatial pattern and overall characteristics of the extreme precipitation events. The widely used data product is TMPA 3-hourly 3B42 which is accumulated to daily and monthly 3B43. The TRMM products are available from 1998 to present with a high spatial resolution (0.25° × 0.25°) over near-global coverage (Huffman *et al.* 2007).

Table 1. Summary of the satellite precipitation products

Satellite Precipitation Products	Spatial Resolution	Temporal Resolution	Temporal Coverage
TRMM	0.25°	1998-Present	Daily/Monthly
PERSIANN-CDR	0.25°	1983-Present	Daily
CHIRPS	0.05°	1981-Present	Daily

Climate Hazards Group InfraRed Precipitation with Station (CHIRPS) data is a long-term (1981-present) near-global (50°S - 50°N) precipitation dataset, developed by jointly the U.S. Geological Survey (USGS) and the Climate Hazards Group (CHG) at the University of California, Santa Barbara. The thermal infrared (TIR) based high resolution ($0.05° \times 0.05°$) CHIRPS data was developed with the main focus to support drought monitoring and forecasting and other land surface modeling activity (Funk *et al.* 2015). CHIRPS has relatively long precipitation records (>30 years) than other available satellite precipitation at daily, pentadal, and monthly temporal resolution (Funk *et al.* 2014). It is a blended product of global precipitation climatology, geostationary TIR satellite estimates, and in-situ gauge observations (Peterson *et al.* 2013). For this study, the monthly CHIRPS version 2.0 precipitation data were used.

Precipitation Estimation from Remotely Sensed Information using Artificial Neural Networks-Climate Data Record (PERSIANN-CDR) is a multi-satellite high-resolution precipitation data developed by the Center for Hydrometeorology and Remote Sensing (CHRS), University of California, Irvine (UCI). The PERSIANN-CDR were generated applying artificial neural network approach on GridSat-B1 infrared (IR) satellite product to provide an estimate of precipitation rate at $0.25° \times 0.25°$ spatial resolution across the near-globe (60°N - 60°S) at a daily temporal resolution as a high-quality Climate Data Record (CDR) of precipitation from 1983 to the near-present (Ashouri *et al.* 2015, Miao *et al.* 2015). The near-global available precipitation data supports many meteorological applications especially extreme events like drought and flood analysis.

3.3. Performance evaluation of satellite precipitation index

10

The time series of monthly precipitation was prepared using spatially aggregated data to quantify the variation between the observed IMD and satellite precipitation products. The annual average difference was calculated to measure the departure and level of underestimation or overestimation of monthly satellite precipitation data from the observed one. For accompaniment, the seasonal climatological variations were derived by temporally aggregating mean for winter (Jan-Feb; JF), pre-monsoon (March-May; MAM), monsoon (June-Sept; JJAS), and post-monsoon (Oct-Dec; OND) seasons during 1998 to 2016 to determine the differences in the seasonal inter-relationship among satellites precipitation datasets.

For a comprehensive evaluation of satellite-precipitation products, a series of widely used statistical metrics such as Pearson's correlation coefficient (CC), Root mean square error (RMSE), Mean Absolute Error (MAE), and Relative Bias (RB) were calculated against observed gauge precipitation data (**Table 2**). CC was derived to test the linear agreement or association between two variables (i.e., how well satellite precipitation data corresponds to the observed precipitation data). Whereas, the RMSE and MAE were used for measuring the average magnitude of estimated error between observed and satellite precipitation. The RB depicted the biasness in the satellite precipitation compared to observed precipitation data. The overall evaluation was performed by pooling all the values from the 39 point for the period of 1998-2016 and then comparing with their respective grid points.

Table 2. List of statistical metrics used in the validation of satellite precipitation products (CHIRPS, PERSIANN-CDR and TRMM), where "O" is observed precipitation, "S" is satellite precipitation, and "n" is sample size

Statistical Metrics	**Equation**	**Optimal Value**	**Unit**

CC	$r = \dfrac{\sum_{i=1}^{n}(O_i - \overline{O})(S_i - \overline{S})}{\sqrt{\sum_{i=1}^{n}(O_i - \overline{O})^2} \cdot \sqrt{\sum_{i=1}^{n}(S_i - \overline{S})^2}}$	1	-
RMSE	$RMSE = \sqrt{\dfrac{1}{n}\sum(S_i - O_i)^2}$	0	mm
MAE	$MAE = \dfrac{1}{n}\sum|S_i - O_i|$	0	mm
Relative Bias	$RB = \dfrac{\sum_{i=1}^{n}(S_i - O_i)}{\sum_{i=1}^{n}(O_i)}$	0	-

3.4. The Standardized Precipitation Index for drought assessment

The SPI computation required fitting a probability distribution such as the Pearson Type III or Gamma probability function for homogenized long-term precipitation records to attain the standard normal variable as normally it follows the nonnormal stable distribution. Then it is transformed into a normal distribution with the unit standard deviation and zero mean for the selected region and desire period through equiprobability transformation (Guttman 1998). In this study, SPI was calculated on a 1, 3, 6, and 12-month time scale using the R platform for evaluation of meteorological drought identified by the IMD and most accurate satellite-precipitation data. The range of SPI is varying between 2 to -2, where negative SPI value indicates drier or drought events and a positive value indicate wet events (**Table 3**).

Table 3. Drought classification based on SPI values (McKee *et al.* 1993)

SPI values	Categories	Probabilities (%)
>2.0	Extremely wet	2.3
1.5 to 1.99	Very wet	4.4
1.0 to 1.49	Moderately wet	9.2

-0.99 to 0.99	Near normal	68.2
-1.0 to -1.49	Moderately dry	9.2
-1.5 to -1.99	Severe dry	4.4
<-2.0	Extremely dry	2.3

3.5. Time series (ARIMA) model development for drought forecasting

The long-term SPI3 time series analysis was performed for modeling the temporal pattern of drought using the Auto Regressive Moving Average (ARIMA) model. Appropriate calibration and validation were performed in the R programming environment. With the calibrated parameters, the best fit ARIMA model was identified, which was then used to predict the upcoming drought condition for the study area. ARIMA is used for the time series analysis and thereby forecasting. The ARIMA model is mainly of two types: 1) non-seasonal linear ARIMA models that defined by parameters as ARIMA (p, d, q), and 2) multiplicative seasonal ARIMA model that is defined by adding seasonal parameters as ARIMA (p, d, q) (P, D, Q). The non-seasonal ARIMA model is mathematically expressed as (Wei 2006, Brockwell and Davis 2016):

$$\phi(B)\nabla^d Z_t = \theta(B)a_t \tag{1}$$

where, $\phi(B)$ and $\theta(B)$ are polynomials for p and q order, respectively and computed as:

$$\theta(B) = 1 - \theta_1 B - ... - \theta_q B^q$$
$$\phi(B) = 1 - \phi_1 B - ... - \phi_p B^p \tag{2}$$

However, the seasonal multiplicative ARIMA model can be written as:

$$\phi_p(B)\Phi_P(B^s)\nabla^d\nabla_s^D Z_t = \theta_q(B)\Theta_Q(B^s)a_t \tag{3}$$

where, p, d, and q are the non-seasonal parameters of the model, which denotes the order of AR model, degree of differencing and the order of the MA model and P, D, Q, and *s* are the

13

order of seasonal AR, seasonal differencing, order of seasonal MA model and the length of the season respectively. ϕ_p, Φ_P, θ_q, and Θ_Q are polynomials coefficients.

The ARIMA model development consists of three stages: identification, estimation, and diagnostic measures (McCleary *et al.* 1980, Chatfield 2000, Box *et al.* 2015). In the first stage of developing the ARIMA model, exploration of time series stationarity was done. After achieving stationarity, the general form of model determined by the autocorrelation function (ACF) and partial autocorrelation functions (PACF) (http://people.duke.edu). Again, the final model is selected based on penalty function statistics the Akaike information criterion (AIC) and Bayesian Information Criterion (BIC) or Schwarz-Bayesian criterion (SBC) using the following formula (Akaike 1974, Schwarz 1978);

$$AIC = -2\log(L) + 2k \qquad (4)$$

$$BIC = -2\log(L) + k\ln(n) \qquad (5)$$

where k= (p+q+P+Q) is the parameters in the model, L denotes the likelihood function of the model, and n is the number of observations.

During model parameter estimation, least-square and moment, conditional sum-of-squares, or maximum likelihood functions (Wilson 1989) were applied, where the statistical significance was qualified using various statistics like standard error, p-values, t-statistics, and z-values. In the last stage of model development, the diagnosis of the ARIMA model was done to ensure the residuals are white noise. Diagnostic statistical tests and plots of residuals were used in estimating the correlation between residuals and white noise such as ACF of residuals (RACF), normal probability of residuals, Periodogram check, histograms of residuals, residuals distribution around the mean, Kolgomorov–Smirnov (K–S) tests, Ljung Box test, etc. (Box and

Pierce 1970, Li 2003). With the calibrated parameters the best-fit model was identified for forecasting.

4. Results and Discussion

4.1. Precipitation Evaluation

The monthly time series of observed IMD and satellite-derived precipitations are shown in **Figure 3a**. Although the precipitation from all the satellites follows a similar pattern, a phase shift is observed in the year 2002 between all satellite-derived precipitations and IMD data. The precipitation peaks correspond to the monsoon season indicates overestimation (compared to IMD observed data) of precipitation in each satellite data, which was much higher for TRMM and PERSIANN-CDR than CHIRPS. **Figure 3b** shows the annual averaged monthly difference between the satellite precipitation products and IMD precipitation data. Similar to the previous observations, TRMM shows the highest overestimation (nearly up to 50 mm) in almost every year except 1998, 2003, 2007, 2009, and 2010; whereas, the PERSIANN-CDR shows the highest difference. In comparison, CHIRPS data shows the lowest overestimation in all the years except a slight underestimation (-0.3 mm) in 2003. At seasonal scale, the significant overestimation in precipitation was observed during the monsoon season, which is lowest for CHIRPS followed by PERSIANN-CDR and TRMM (**Figure 3c**).

The statistical comparison between the observed IMD and satellite precipitation was carried out for individual IMD grids (39 grids) in the study area. The plots of different statistical metrics between observed and three different satellite precipitation estimates are shown in **Figure 4**. All the satellite precipitation products showed good agreement with the correlation coefficient (CC)

values ranging from 0.75 to 0.94. Relatively higher CC was obtained for TRMM with maximum, minimum, and average values as 0.94, 0.79, and 0.88, respectively, followed by PERSIANN-CDR (0.93, 0.76, and 0.88) and CHIRPS (0.92, 0.75 and 0.87) (**Figure 4a**).
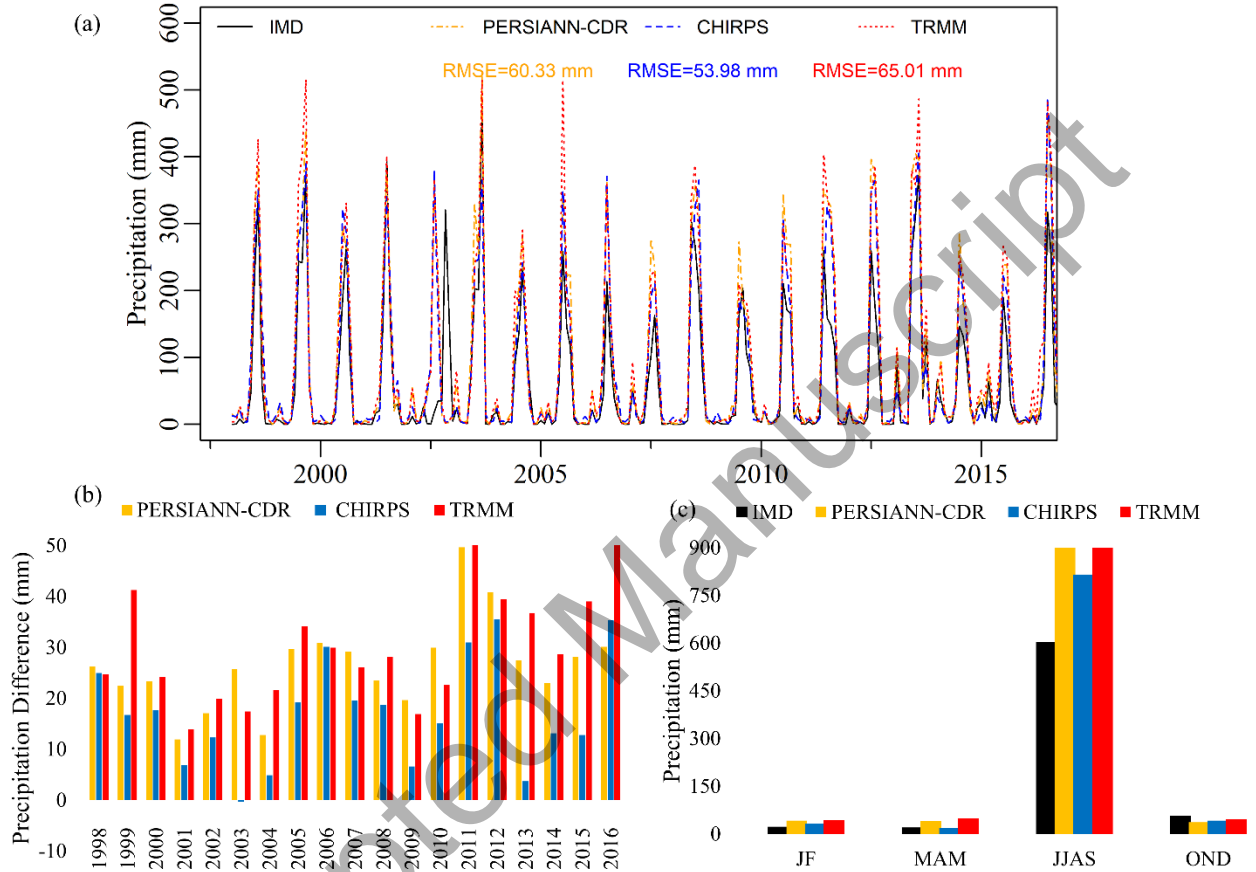

Figure 3. The monthly time series (a), Annual averaged difference (b), and Seasonal variations (c) between IMD precipitation and three satellite precipitation products

However, all satellite precipitation data seems to overestimate the monthly observed precipitation for all the points except 13 where the PERSIANN-CDR underestimated the precipitation. CHIRPS showed a minimum relative bias (0.58) in comparison to TRMM (0.81) and PERSIANN-CDR (0.99) (**Figure 4b**). Similarly, the MAE and RMSE for CHIRPS data were minimum having the average value of 31.99 mm month^{-1} and 60.68 mm month^{-1}, respectively. Whereas, the MAE values for PERSIANN-CDR and TRMM were estimated as

35.90 mm month^{-1} and 37.60 mm month^{-1} with the RMSE values of 67. 35 mm month^{-1} and

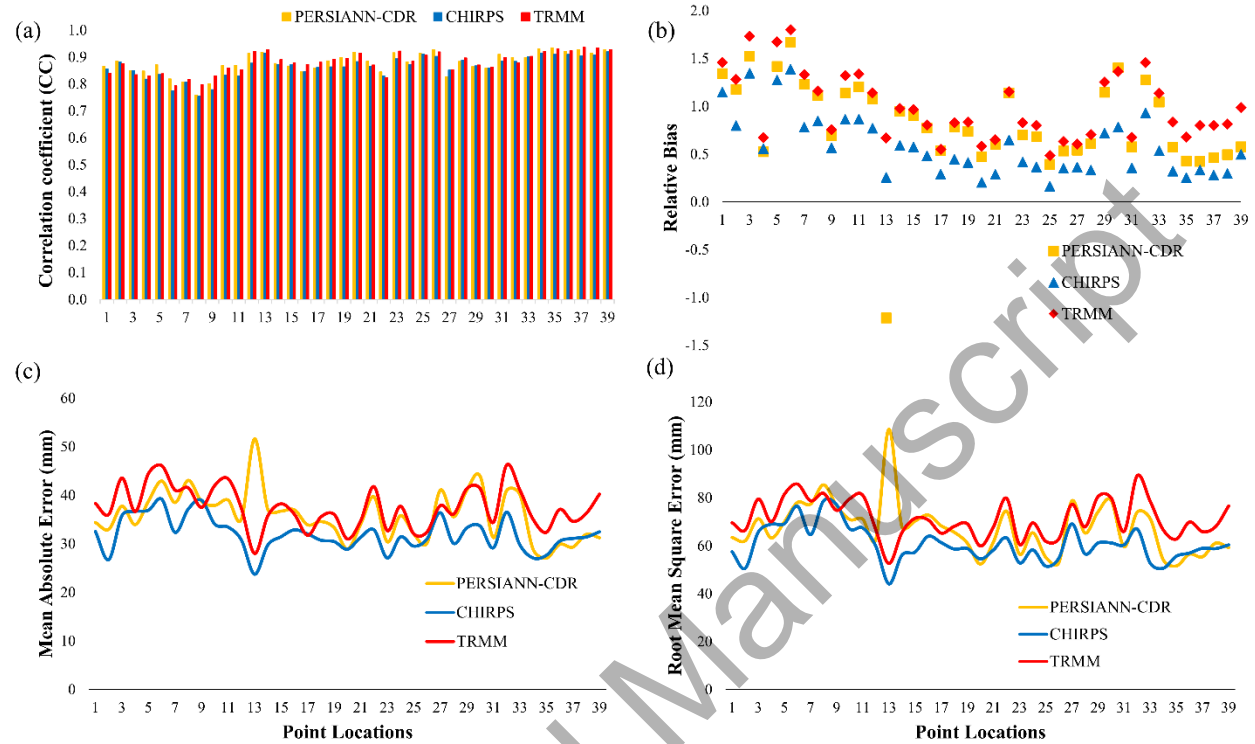71.57 mm month^{-1}, respectively (**Figure 4c, d**).

Figure 4. The statistical metrics- correlation coefficient (a), Relative bias (b), Mean absolute

error (c), and Root mean square error (d)- for the selected 39 points in the study area.

The scatter plot between observed IMD precipitation and the three satellite products (TRMM,

CHIRPS, and PERSIANN-CDR) for the nineteen-year monthly precipitation for 39 grids over

the Bundelkhand region is shown in **Figure 5**. All satellite products showed a significant (p<

0.0001) coefficient of determinants (R^2), which was slightly higher for TRMM (0.78) followed

by PERSIANN-CDR (0.77) than CHIRPS (0.75). However, the regression line (black) exhibited

the closest agreement with 1:1 line (red-dotted) for CHIRPS followed by PERSIANN-CDR and

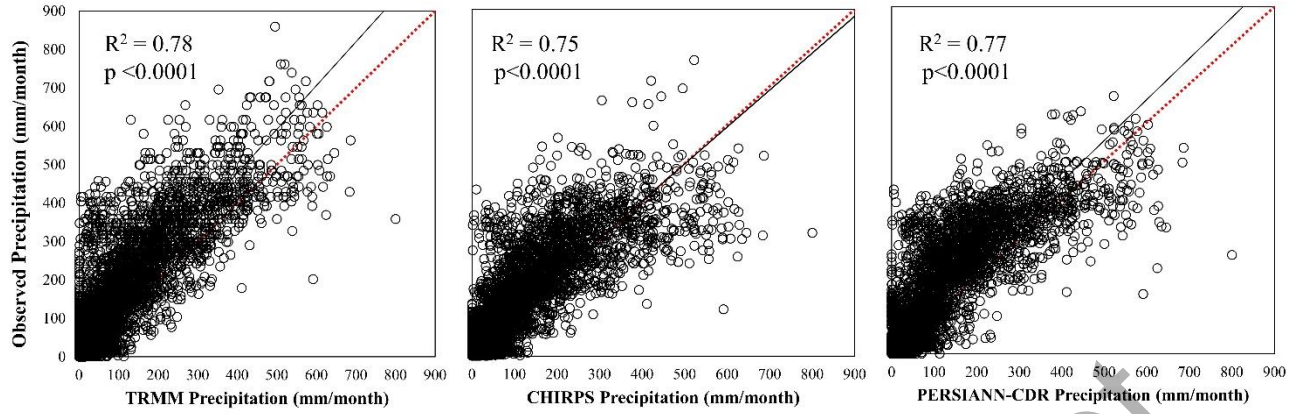TRMM, indicating their deviation from the observed data.

Figure 5. Scatter plots between the observed IMD precipitation and satellite-based precipitation at a monthly time scale. Linear regression is fitted with sample size (n) 8892. The dotted red line indicates 1:1 and the black line indicates the best fit linear regression line.

The overall performance of all three satellite products is promising for identifying precise satellite precipitation products that could potentially be utilized in meteorological and other allied studies (**Table 4**). However, the statistical comparison shows a comparatively better correlation coefficient for TRMM and PERSIANN-CDR in almost all the points, the CHIRPS exhibits the lowest error in terms of MAE, RMSE, and bias that indicates better performance of CHIRPS in comparison to TRMM and PERSIANN-CRD. Thus, we have selected high-resolution CHIRPS data in this study for meteorological drought assessment and forecasting.

Table 4. Summary of statistical metrics

Data sets	PERSIANN-CDR	CHIRPS	TRMM
R^2	0.77	0.75	0.78
CC	0.88	0.87	0.88
RB	0.81	0.58	0.99
MAE	35.90	32.00	37.60
RMSE	67.35	60.68	71.57

18

4.2. SPI Comparison

Additionally, we corroborated the suitability of CHIRPS in drought monitoring. The spatially averaged SPI has been calculated using the domain-averaging process at different timescales as SPI1, SPI3, SPI6, and SPI12 to compare with IMD derived SPI from 1998 to 2016 (**Figure 6**). Short duration SPI computation evaluates the impact of drought on agriculture, while longer duration SPI is most suitable for detecting hydrological drought hazard (Vicente-Serrano *et al.* 2014). We observed close agreements and consistency between CHIRPS and IMD data derived SPI values in terms of both frequency and intensity. The performance of CHIRPS was observed well in capturing drought for all the time scales.
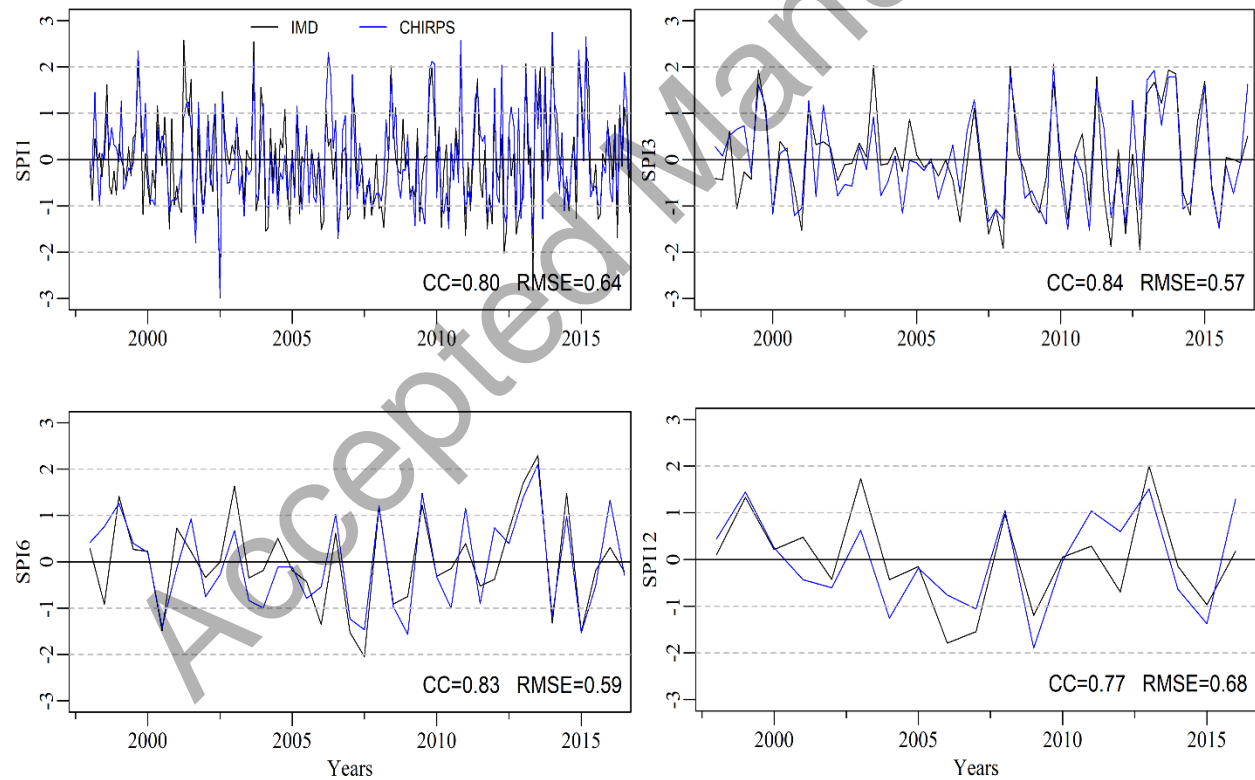

Figure 6. The SPI time series for comparison between CHIRPS and observed IMD precipitation from 1998 to 2016 at different time scales: (a) 1-month; (b) 3-month; (c) 6-month; and (d) 12-month.
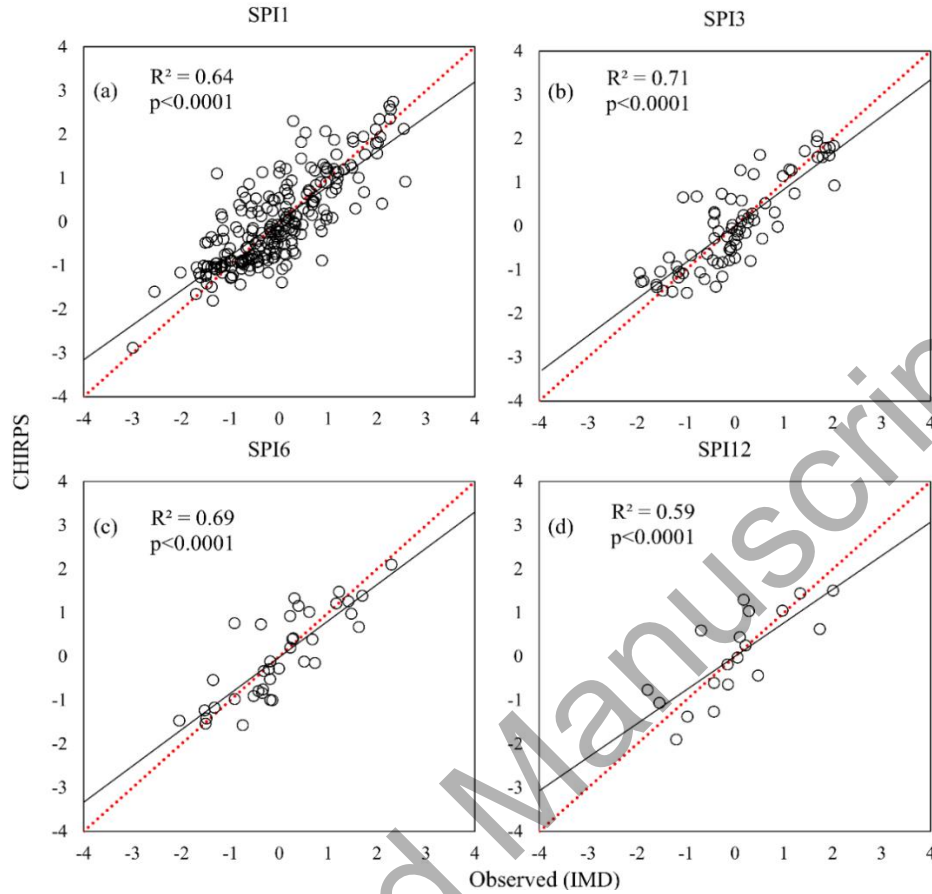
19

Figure 7. Scatter plots between CHIRPS and observed IMD derived SPI from 1998 to 2016 at different time scales: (a) 1-month; (b) 3-month; (c) 6-month; and (d) 12-month.

It identifies the historic drought events, which was occurred in most of the Indian regions in the years 2002, 2009, 2014, and 2015 (www.iwmi.cgiar.org; www.im4change.org),(Gupta and Head, Samra 2004). The correlation coefficient (CC) between IMD and CHIRPS derived SPIs were estimated as > 0.75 and RMSEs < 0.70 for all time scales. A comparative study among all the time scale exhibits better agreements for SPI3 and SPI6 (CC: 0.84 and 0.83 respectively; and RMSE: 0.57 and 0.59, respectively). On the contrary, SPI1 and SPI12 showed comparatively moderate and lower agreement (CC: 0.8 and 0.77, respectively, and RMSE: 0.64 and 0.68, respectively). The scatter plot between IMD and CHIRPS data derived SPI at different time

scales shown in **Figure 7.** All SPI timescale showed significant R^2 with (p<0.0001), which was comparatively higher for SPI3 (0.71).

4.3. Meteorological drought assessment based on CHIRPS during Monsoon Season

Majority of the precipitation in this region is concentrated in monsoon season (June-September, JJAS). With the availability of CHIRPS data science 1981, SPI3 was evaluated for the monsoon season from 1981 to 2016 (36 years) to assess the drought pattern and severity in this region (Figure 8). The obtained results identified seven severe to extreme drought events in the study region during 1981 to 2016 (**Figure 8**). With reference to past studies, the years 1982, 1984, 1987, and 2014-2015 undergone through severe drought event, while years 1992, 2002, and 2009 faces extreme drought conditions with an intensity ranging from -1.75 to -1.87 and -2.21 to -2.30, respectively. The current study findings are consistent with Thomas *et al.* (2015).
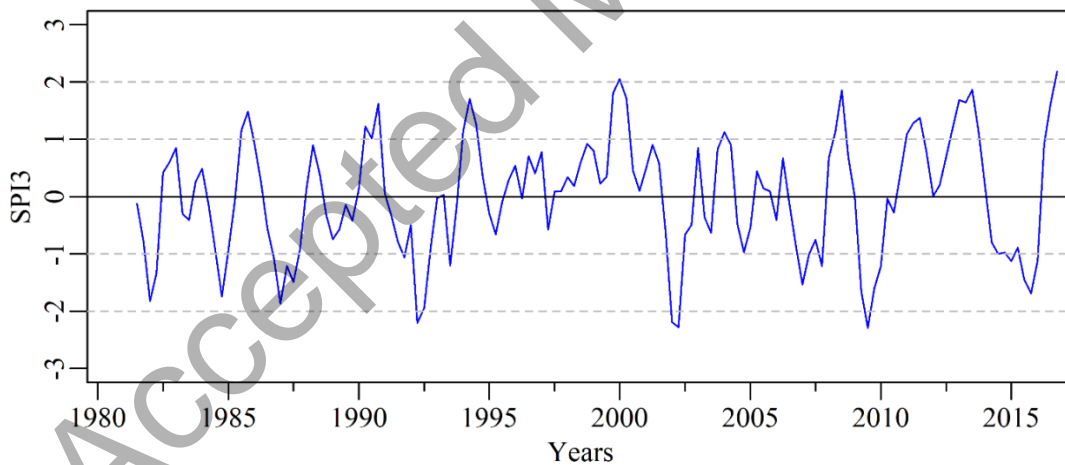

Figure 8. SPI3 time series based on all grids average over the Bundelkhand region.

4.4. SPI Time Series Modeling

4.4.1. Model Development

The ARIMA model was used to analyze the temporal patterns and forecast the drought events through CHIRPS data derived SPI at the 3-month time scale (SPI3). The seasonal datasets (June-September or JJAS) from 1981 to 2011 were used for model development and calibration, while 2012 to 2016 were used for the validation of the model.

Model Identification: The ACF and PACF plots generated using the SPI3 time series data are shown in **Figure 9**, suggest the input data series to be stationary. Again, the stationarity of the data series was also confirmed by applying the Dickey-Fuller Test ($p = 0.01$). The ACF shows a sine-wave shape with the first three significant lags and PACF with the first two significant lags, which indicates the applicability of both AR and MA components. Considering this, ARIMA (p, 0, q) model were identified with possible $p = 1$ to 2 and $q = 1$ to 3. All the possible combinations were tested and compared to identify the best fit model based on minimum AIC and SBC/BIC values, which indicates white noise residuals. **Table 5** shows the different combinations of the model with estimated AIC and BIC values.
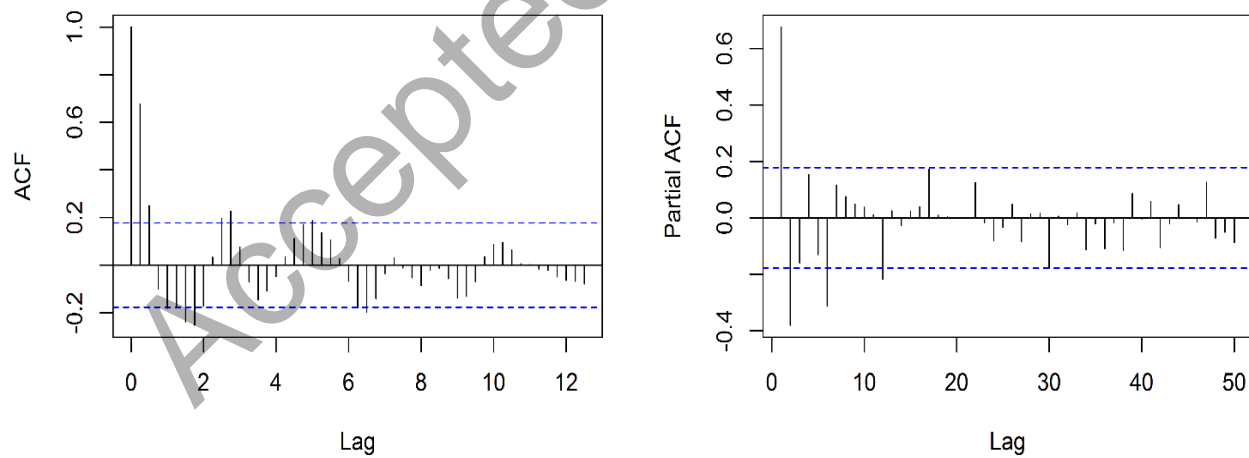

Figure 9. ACF and PACF plots used for model selection for the SPI3 series.

Table 5. Comparison of AIC and BIC for the selection of a best-fit model for SPI3.

ARIMA Models	AIC	BIC/SBC
ARIMA (2,0,0)	254.87	266.08
ARIMA (2,0,1)	254.62	268.63
ARIMA (2,0,2)	241.90	258.71
ARIMA (2,0,3)	242.78	262.41
ARIMA (1,0,3)	238.14	252.95
ARIMA (1,0,2)	243.12	257.13
ARIMA (1,0,1)	262.89	274.10
ARIMA (0,0,3)	241.60	255.62
ARIMA (0,0,2)	243.27	254.48
ARIMA (0,0,2) (0,0,1)	238.84	252.86

Parameter estimation: The second stage of model development is the estimation of parameters using the maximum likelihood method in this study. The z-values, p-values, and standard error corresponds to each parameter were evaluated to test the statistical significance of the parameters. Usually, p-values are informative by itself and state parameters are significant if its value is less than 0.05 at a 95% confidence interval. The summary of the statistical parameters of the best fit model has been given in **Table 6**.

Table 6. Summary of the statistical parameters of ARIMA (1,0,3).

Model Parameters	Variables in the model			
	Estimate value	**Standard error**	**Z-value**	**P <0.05**
AR1	-0.7483	0.1221	-6.1327	0.00
MA1	1.7199	0.1052	16.3337	0.00
MA2	1.5066	0.1294	11.6376	0.00
MA3	0.7307	0.0808	9.0351	0.00
Intercept	-0.0383	0.1541	-0.2487	

Diagnostic measures: This step of model development involves verification of the adequacy of the selected model using diagnostic statistics and plots of residuals. In the present study, the residual ACF function (RACF), histogram of residuals, Ljung Box test, and normal probability

of residuals test were performed for residual checking. In RACF plot, the correlogram was drawn by plotting residual ACF (r_k) against lag k. The ACF of residuals for the ARIMA (1,0,3) model is shown in **Figure 10a**, indicates that all values were within the significant bounds and shown no significant correlation between residuals except the first lag. Histograms of residuals for the same model are shown in **Figure 10b** shows the normal distribution of residuals that signifies the residuals were white noise. The p-values obtained from the Ljung Box test are shown in **Figure 10c**, represents all values that were well above 0.05, indicating white noise residuals and model adequacy. The normal probability of residuals plot (**Figure 10d**) shows the white noise residuals as it appears fairly linear that holds normality assumptions of the residuals (Durbin 1960, Box and Pierce 1970, McLeod and Li 1983, Chow *et al.* 1988).
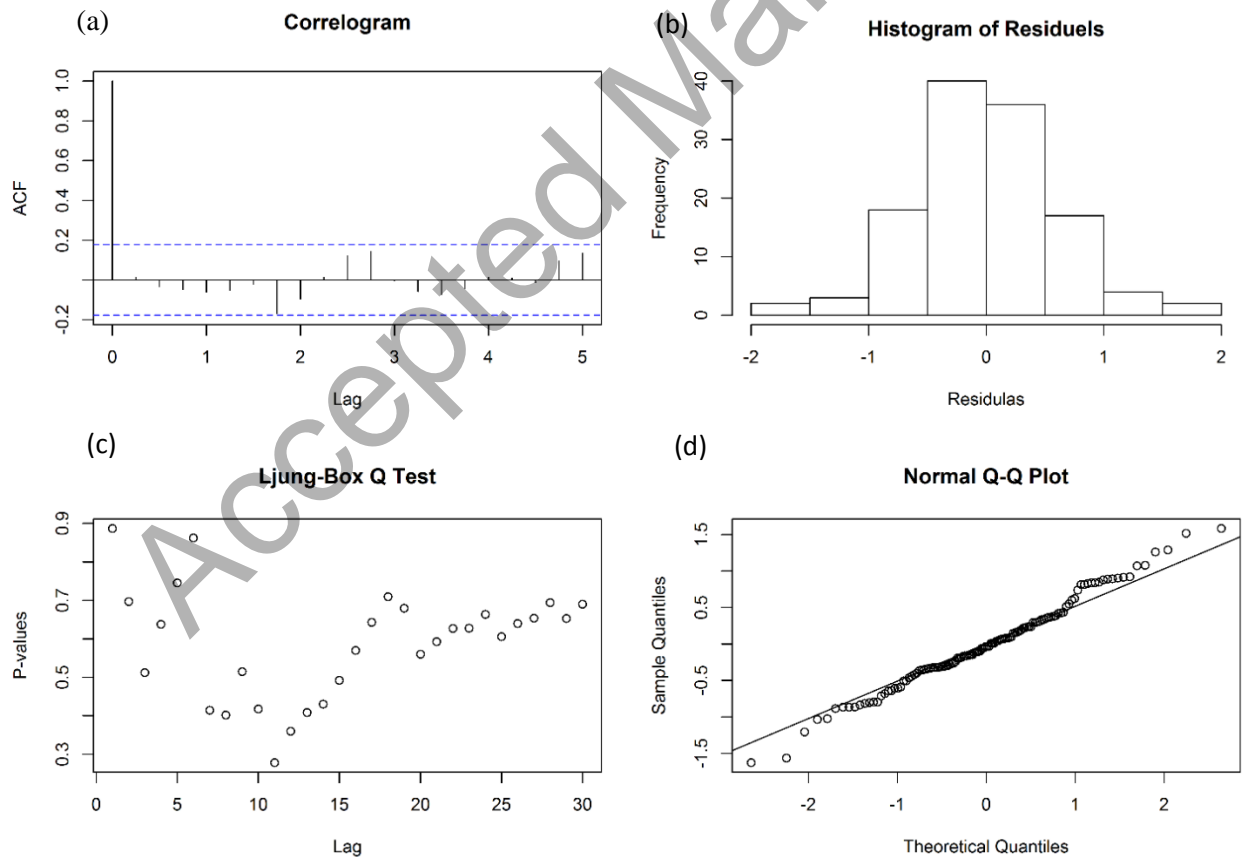

Figure 10. Diagnostic check for best-fitted model ARIMA (1,0,3)

4.4.2. Forecasting

The best fit ARIMA model (1,0,3) was validated with the observed data for the monsoon season (JJAS) from 2012 to 2016. The forecasting was done for one-month lead-time (because it decreases with increasing lead time) for better accuracy, that was also observed in previous studies by (Mishra and Desai 2005), (Fathabadi *et al.* 2009), (Bazrafshan *et al.* 2015) and Han *et al.* (2012). **Figure 11a** represents the observed and modeled SPI time series, which indicates close agreement among modeled (ARIMA) with observed CHIRPS and IMD. The obtained result shows that the forecasted data follows the same pattern and satisfied the basic statistics compared to the monitored and observed data. The high correlations and low RMSE were obtained for both CHIRPS and IMD as shown in (Figure 11b).
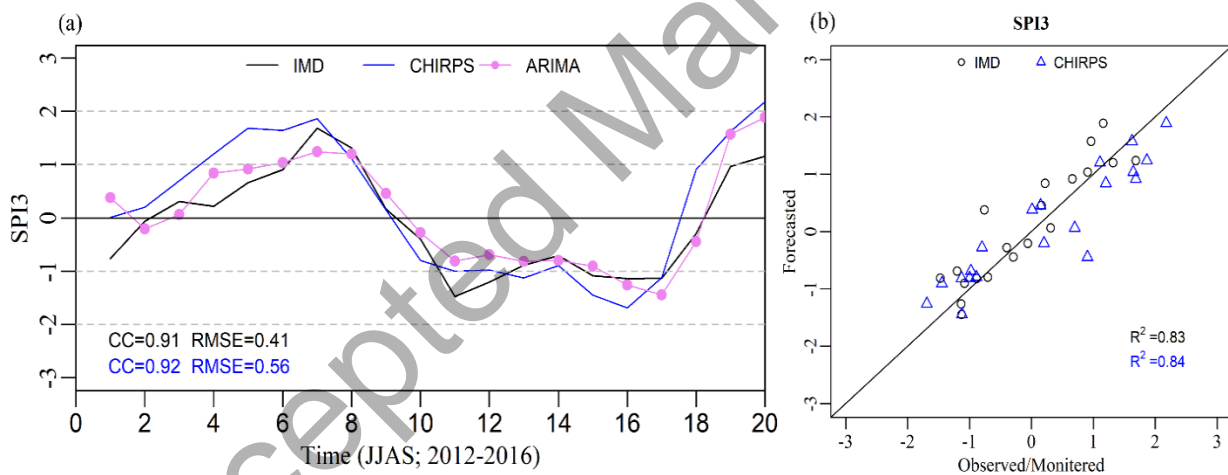
Figure 11. (a) SPI time series and (b) scatter plot for observed (IMD), CHIRPS along with the forecasted data using the ARIMA (1,0,3) model.

5. Discussion

In India, this is the first study which evaluates precipitation products to monitor and forecast drought hazard in the Bundelkhand region, where frequent drought is regularly witnessed by the

community. This study assessed the performance of three widely used satellite-derived precipitation products having long-term records as TRMM, PERSIANN-CDR, and CHIRPS. The ground observed data recorded by IMD over this region was taken as the reference or baseline data for comparison. These evaluations are done for promoting the use of satellite precipitation products for hydro-meteorological, agriculture, natural hazards, and other related studies and planning. The evaluation was carried out on a monthly scale with a common grid size of 0.25º. Additionally, the evaluation includes assessment via a drought index as the Standardized Precipitation Index (SPI). The SPI time series analysis was performed using the ARIMA model to project the SPI for drought hazard preparedness in the study region. Although the precipitation event is dependent on many dynamic and coupled processes, which requires highly complex coupled simulation models for prediction, here the simplistic and reliable time series analysis was performed using the ARIMA model. Mishra and Desai (2005), Modarres, (2007), Han et al. (2010), Alam et al. (2014), etc. studied and assessed the applicability of the ARIMA model for reliable time series forecasting of drought. Karimi et al. (2019) confirmed the robustness of ARIMA model in the semi-arid region of Iran by forecasting the SPI3 time series and observed a fairly good agreement (CC >0.7 and RMSE <0.4) with the observed data.

The comparison of the three multi-satellite precipitation products shows that all the three precipitation products had almost similar accuracies (correlations ranges from 0.75 to 0.94) but notable low relative bias and RMSE values (0.58 and 60.6 mm month^{-1}) were observed with CHIRPS data. Therefore, we concluded that the satellite precipitation records is well captured by the CHIRPS data in comparison to the other two satellite precipitations data used in the study region. Recent studies at India level by (Prakash 2019) indicates a higher error (high bias and RMSE, and lower correlation) in satellite precipitation data (including CHRIPS) over a tropical

26

and mountainous region. Over the central India region, (Prakash 2019) estimated the CC as 0.99 with RMSE of 0.84 (mm day^{-1}) and bias ratio of 1.11. Moreover, many studies have been also indicated CHIRPS as the best data for drought monitoring with relatively lower error and high correlation after comparing it with gauge precipitation data (Bayissa *et al.* 2017, Shrestha *et al.* 2017).

The reasonably good results of CHIRPS are probably due to its higher spatial resolutions (as 0.05° in comparison to other data having a spatial resolution of 0.25°) and integration of more in-situ data in a two-phase process with high-resolution climatology and multi-satellite products. It may be indicated that higher resolution data is proportional to accuracy depending on the method adopted for data processing (Dandridge *et al.* 2019). This study confirms that CHIRPS precipitation can be used as an alternative to IMD data for studying hydro-meteorological phenomena such as long-term drought assessment even at a local scale and suitable for ungagged basin. This infers regions with sparse rain-gauge stations and data records having inconsistency in the recording can blend the CHIRPS precipitation data to fill the spatial and temporal data gaps.

6. Conclusions

Drought monitoring and assessment for improved management strategies and policy development are lacking in numbers of underprivileged drought-prone and economically backward regions in India. Such studies are exaggerated by the unavailability of suitable rain-gauge station data. The current study investigated the effectiveness of the three satellite-derived precipitation products to monitor and forecast drought events in the Bundelkhand region of India. Rainfed agriculture-dependent Bundelkhand region of central India is adversely affected by recurrent and severe drought conditions, which becomes worst due to poor management

strategies and water scarcity. Results showed that the high resolution (0.05°) CHIRPS data is the most suitable for drought characterization according to statistical performance studied from 1998 to 2016 in comparison to (PERSIANN-CDR, CHIRPS, and TRMM). The monthly CHIRPS data was used to evaluate the drought condition for 36 years (1981-2016) at 3- month time scale (SPI3). This research also examined the feasibility of applying the ARIMA time series model using SPI3 for drought forecasting. In total, seven distinct drought events were found in the region during the period from 1981 to 2016, in which four can be placed into severe droughts (in the year 1982, 1984, 1987, and 2015) and three into extremes drought (in the year 1992, 2002 and 2009) categories. Based on the high accuracy of ARIMA, the forecasting was carried out at a one-month lead-time. The outcome of the study can be used for the sustainable water resources management and other watershed management related activities in the region and could be applied to other regions with similar hydro-climatic conditions.

Conflict of Interest: None

References

Akaike, H., 1974. A new look at the statistical model identification. *Selected papers of hirotugu akaike.* Springer, 215-222.

Alijanian, M., Rakhshandehroo, G.R., Mishra, A.K. & Dehghani, M., 2017. Evaluation of satellite rainfall climatology using cmorph, persiann-cdr, persiann, trmm, mswep over iran. *International Journal of Climatology,* 37 (14), 4896-4914.

Ashouri, H., Hsu, K.-L., Sorooshian, S., Braithwaite, D.K., Knapp, K.R., Cecil, L.D., Nelson, B.R. & Prat, O.P., 2015. Persiann-cdr: Daily precipitation climate data record from

multisatellite observations for hydrological and climate studies. *Bulletin of the American Meteorological Society,* 96 (1), 69-83.

Awange, J., Ferreira, V., Forootan, E., Andam-Akorful, S., Agutu, N. & He, X., 2016. Uncertainties in remotely sensed precipitation data over africa. *International Journal of Climatology,* 36 (1), 303-323.

Bandyopadhyay, N., Bhuiyan, C. & Saha, A., 2020. Drought mitigation: Critical analysis and proposal for a new drought policy with special reference to gujarat (india). *Progress in Disaster Science,* 5, 100049.

Bayissa, Y., Tadesse, T., Demisse, G. & Shiferaw, A., 2017. Evaluation of satellite-based rainfall estimates and application to monitor meteorological drought for the upper blue nile basin, ethiopia. *Remote Sensing,* 9 (7), 669.

Bazrafshan, O., Salajegheh, A., Bazrafshan, J., Mahdavi, M. & Fatehi Maraj, A., 2015. Hydrological drought forecasting using arima models (case study: Karkheh basin). *Ecopersia,* 3 (3), 1099-1117.

Beck, H.E., Vergopolan, N., Pan, M., Levizzani, V., Van Dijk, A.I., Weedon, G.P., Brocca, L., Pappenberger, F., Huffman, G.J. & Wood, E.F., 2017. Global-scale evaluation of 22 precipitation datasets using gauge observations and hydrological modeling. *Hydrology and Earth System Sciences,* 21 (12), 6201-6217.

Box, G.E., Jenkins, G.M., Reinsel, G.C. & Ljung, G.M., 2015. *Time series analysis: Forecasting and control*: John Wiley & Sons.

Box, G.E. & Pierce, D.A., 1970. Distribution of residual autocorrelations in autoregressive-integrated moving average time series models. *Journal of the American statistical Association,* 65 (332), 1509-1526.

Brockwell, P.J. & Davis, R.A., 2016. *Introduction to time series and forecasting*: springer.

Chatfield, C., 2000. *Time-series forecasting*: Chapman and Hall/CRC.

Chen, S., Zhang, L., Zhang, Y., Guo, M. & Liu, X., 2020. Evaluation of tropical rainfall measuring mission (trmm) satellite precipitation products for drought monitoring over the middle and lower reaches of the yangtze river basin, china. *Journal of Geographical Sciences,* 30 (1), 53-67.

Chow, V.T., Maidment, D.R. & Mays, L.W., 1988. *Applied hydrology*.

Contreras, J., Espinola, R., Nogales, F.J. & Conejo, A.J., 2003. Arima models to predict next-day electricity prices. *IEEE transactions on power systems,* 18 (3), 1014-1020.

Dandridge, C., Lakshmi, V., Bolten, J. & Srinivasan, R., 2019. Evaluation of satellite-based rainfall estimates in the lower mekong river basin (southeast asia). *Remote Sensing,* 11 (22), 2709.

Durbin, J., 1960. The fitting of time-series models. *Revue de l'Institut International de Statistique,* 233-244.

Fang, J., Yang, W., Luan, Y., Du, J., Lin, A. & Zhao, L., 2019. Evaluation of the trmm 3b42 and gpm imerg products for extreme precipitation analysis over china. *Atmospheric research,* 223, 24-38.

Fathabadi, A., Gholami, H., Salajeghe, A., Azanivand, H. & Khosravi, H., 2009. Drought forecasting using neural network and stochastic models. *Advances in Natural and Applied Sciences,* 3 (2), 137-146.

Fereidoon, M., Koch, M. & Brocca, L., 2019. Predicting rainfall and runoff through satellite soil moisture data and swat modelling for a poorly gauged basin in iran. *Water,* 11 (3), 594.

Fernández, C., Vega, J.A., Fonturbel, T. & Jiménez, E., 2009. Streamflow drought time series forecasting: A case study in a small watershed in north west spain. *Stochastic Environmental Research and Risk Assessment,* 23 (8), 1063.

Funk, C., Peterson, P., Landsfeld, M., Pedreros, D., Verdin, J., Shukla, S., Husak, G., Rowland, J., Harrison, L. & Hoell, A., 2015. The climate hazards infrared precipitation with stations—a new environmental record for monitoring extremes. *Scientific data,* 2, 150066.

Funk, C.C., Peterson, P.J., Landsfeld, M.F., Pedreros, D.H., Verdin, J.P., Rowland, J.D., Romero, B.E., Husak, G.J., Michaelsen, J.C. & Verdin, A.P., 2014. A quasi-global precipitation time series for drought monitoring. *US Geological Survey data series,* 832 (4), 1-12.

Gao, Y. & Liu, M., 2012. Evaluation of high-resolution satellite precipitation products using rain gauge observations over the tibetan plateau. *Hydrology & Earth System Sciences Discussions,* 9 (8).

Glantz, M.H., 1994. *Drought follows the plow: Cultivating marginal areas*: Cambridge University Press.

Gupta, A.K. & Head, N., Vulnerability assessment and mitigation analysis for drought in bundelkhand region.

Gupta, A.K., Nair, S.S., Ghosh, O., Singh, A. & Dey, S., 2014. Bundelkhand drought: Retrospective analysis and way ahead. *National Institute of Disaster Management, New Delhi,* 148.

Gupta, V., Kumar Jain, M. & Singh, V.P., 2020. Multivariate modeling of projected drought frequency and hazard over india. *Journal of Hydrologic Engineering,* 25 (4), 04020003.

Guttman, N.B., 1998. Comparing the palmer drought index and the standardized precipitation index 1. *JAWRA Journal of the American Water Resources Association,* 34 (1), 113-121.

Hamilton, J.D., 1994. *Time series analysis*: Princeton university press Princeton, NJ.

Han, P., Wang, P., Tian, M., Zhang, S., Liu, J. & Zhu, D., Year. Application of the arima models in drought forecasting using the standardized precipitation indexed.^eds. *International Conference on Computer and Computing Technologies in Agriculture*Springer, 352-358.

Hao, Z. & Singh, V.P., 2015. Drought characterization from a multivariate perspective: A review. *Journal of Hydrology,* 527, 668-678.

Heim Jr, R.R., 2002. A review of twentieth-century drought indices used in the united states. *Bulletin of the American Meteorological Society,* 83 (8), 1149-1165.

Hirpa, F.A., Gebremichael, M. & Hopson, T., 2010. Evaluation of high-resolution satellite precipitation products over very complex terrain in ethiopia. *Journal of Applied Meteorology and Climatology,* 49 (5), 1044-1051.

Huffman, G.J., Bolvin, D.T., Nelkin, E.J., Wolff, D.B., Adler, R.F., Gu, G., Hong, Y., Bowman, K.P. & Stocker, E.F., 2007. The trmm multisatellite precipitation analysis (tmpa): Quasi-global, multiyear, combined-sensor precipitation estimates at fine scales. *Journal of hydrometeorology,* 8 (1), 38-55.

Jentsch, A. & Beierkuhnlein, C., 2008. Research frontiers in climate change: Effects of extreme meteorological events on ecosystems. *Comptes Rendus Geoscience,* 340 (9-10), 621-628.

Jiang, S., Ren, L., Hong, Y., Yong, B., Yang, X., Yuan, F. & Ma, M., 2012. Comprehensive evaluation of multi-satellite precipitation products with a dense rain gauge network and optimally merging their simulated hydrological flows using the bayesian model averaging method. *Journal of Hydrology,* 452, 213-225.

Kalisa, W., Zhang, J., Igbawua, T., Ujoh, F., Ebohon, O.J., Namugize, J.N. & Yao, F., 2020. Spatio-temporal analysis of drought and return periods over the east african region using standardized precipitation index from 1920 to 2016. *Agricultural Water Management,* 237, 106195.

Kimani, M., Hoedjes, J. & Su, Z., 2017. An assessment of satellite-derived rainfall products relative to ground observations over east africa. *Remote sensing,* 9 (5), 430.

Li, W.K., 2003. *Diagnostic checks in time series*: Chapman and Hall/CRC.

Liu, Z., Ostrenga, D., Teng, W. & Kempler, S., 2012. Tropical rainfall measuring mission (trmm) precipitation data and services for research and applications. *Bulletin of the American Meteorological Society,* 93 (9), 1317-1325.

Maca, P. & Pech, P., 2016. Forecasting spei and spi drought indices using the integrated artificial neural networks. *Computational intelligence and neuroscience,* 2016.

Mccleary, R., Hay, R.A., Meidinger, E.E. & Mcdowall, D., 1980. *Applied time series analysis for the social sciences*: Sage Publications Beverly Hills, CA.

Mckee, T.B., Doesken, N.J. & Kleist, J., Year. The relationship of drought frequency and duration to time scalesed.^eds. *Proceedings of the 8th Conference on Applied Climatology*American Meteorological Society Boston, MA, 179-183.

Mcleod, A.I. & Li, W.K., 1983. Diagnostic checking arma time series models using squared-residual autocorrelations. *Journal of time series analysis,* 4 (4), 269-273.

Miao, C., Ashouri, H., Hsu, K.-L., Sorooshian, S. & Duan, Q., 2015. Evaluation of the persiann-cdr daily rainfall estimates in capturing the behavior of extreme precipitation events over china. *Journal of Hydrometeorology,* 16 (3), 1387-1396.

Mishra, A. & Desai, V., 2005. Drought forecasting using stochastic models. *Stochastic Environmental Research and Risk Assessment,* 19 (5), 326-339.

Mishra, A. & Desai, V., 2006. Drought forecasting using feed-forward recursive neural network. *ecological modelling,* 198 (1-2), 127-138.

Moazami, S., Golian, S., Kavianpour, M.R. & Hong, Y., 2013. Comparison of persiann and v7 trmm multi-satellite precipitation analysis (tmpa) products with rain gauge data over iran. *International journal of remote sensing,* 34 (22), 8156-8171.

Morid, S., Smakhtin, V. & Bagherzadeh, K., 2007. Drought forecasting using artificial neural networks and time series of drought indices. *International Journal of Climatology: A Journal of the Royal Meteorological Society,* 27 (15), 2103-2111.

Naresh Kumar, M., Murthy, C., Sesha Sai, M. & Roy, P., 2009. On the use of standardized precipitation index (spi) for drought intensity assessment. *Meteorological applications,* 16 (3), 381-389.

Pai, D., Sridhar, L., Rajeevan, M., Sreejith, O., Satbhai, N. & Mukhopadhyay, B., 2014. Development of a new high spatial resolution (0.25× 0.25) long period (1901−2010) daily gridded rainfall data set over india and its comparison with existing data sets over the region. *Mausam,* 65 (1), 1-18.

Pandey, V., Maurya, S. & Srivastava, P.K., 2019. Assessment of agricultural drought using a climate change initiative (cci) soil moisture derived/soil moisture deficit: Case study from bundelkhand. *Wastewater Reuse and Watershed Management: Engineering Implications for Agriculture, Industry, and the Environment*, 63.

Pandey, V. & Srivastava, P., 2018. Integration of satellite, global reanalysis data and macroscale hydrological model for drought assessment in sub-tropical region of india. *Int. Arch. Photogramm. Remote Sens. Spat. Inf. Sci,* 42.

Pandey, V. & Srivastava, P.K., Year. Evaluation of satellite precipitation data for drought monitoring in bundelkhand region, indiaed.^eds. *IGARSS 2019-2019 IEEE International Geoscience and Remote Sensing Symposium*IEEE, 9910-9913.

Pandey, V. & Srivastava, P.K., 2019b. Integration of microwave and optical/infrared derived datasets for a drought hazard inventory in a sub-tropical region of india. *Remote Sensing,* 11 (4), 439.

Peña-Arancibia, J.L., Van Dijk, A.I., Renzullo, L.J. & Mulligan, M., 2013. Evaluation of precipitation estimation accuracy in reanalyses, satellite products, and an ensemble method for regions in australia and south and east asia. *Journal of Hydrometeorology,* 14 (4), 1323-1333.

Peterson, P., Funk, C., Husak, G., Pedreros, D., Landsfeld, M., Verdin, J. & Shukla, S., Year. The climate hazards group infrared precipitation (chirp) with stations (chirps): Development and validationed.^eds. *AGU Fall Meeting Abstracts*.

Prakash, S., 2019. Performance assessment of chirps, mswep, sm2rain-cci, and tmpa precipitation products across india. *Journal of hydrology,* 571, 50-59.

Samra, J., 2004. *Review and analysis of drought monitoring, declaration and management in india*: IWMI.

Schwarz, G., 1978. Estimating the dimension of a model. *The annals of statistics,* 6 (2), 461-464.

Sharifi, E., Steinacker, R. & Saghafian, B., 2016. Assessment of gpm-imerg and other precipitation products against gauge data under different topographic and climatic conditions in iran: Preliminary results. *Remote Sensing,* 8 (2), 135.

Shen, Y., Xiong, A., Wang, Y. & Xie, P., 2010. Performance of high-resolution satellite precipitation products over china. *Journal of Geophysical Research: Atmospheres,* 115 (D2).

Shrestha, N.K., Qamer, F.M., Pedreros, D., Murthy, M., Wahid, S.M. & Shrestha, M., 2017. Evaluating the accuracy of climate hazard group (chg) satellite rainfall estimates for precipitation based drought monitoring in koshi basin, nepal. *Journal of Hydrology: Regional Studies,* 13, 138-151.

Sirdaş, S. & Sen, Z., 2003. Spatio-temporal drought analysis in the trakya region, turkey. *Hydrological Sciences Journal,* 48 (5), 809-820.

Stisen, S. & Sandholt, I., 2010. Evaluation of remote-sensing-based rainfall products through predictive capability in hydrological runoff modelling. *Hydrological Processes: An International Journal,* 24 (7), 879-891.

Thomas, T., Jaiswal, R., Galkate, R. & Nayak, T., 2016. Reconnaissance drought index based evaluation of meteorological drought characteristics in bundelkhand. *Procedia Technology,* 24, 23-30.

Thomas, T., Nayak, P. & Ghosh, N.C., 2015. Spatiotemporal analysis of drought characteristics in the bundelkhand region of central india using the standardized precipitation index. *Journal of Hydrologic Engineering,* 20 (11), 05015004.

Umran Komuscu, A., 1999. Using the spi to analyze spatial and temporal patterns of drought in turkey. *Drought Network News (1994-2001)*, 49.

Vicente-Serrano, S.M., Lopez-Moreno, J.-I., Beguería, S., Lorenzo-Lacruz, J., Sanchez-Lorenzo, A., García-Ruiz, J.M., Azorin-Molina, C., Morán-Tejeda, E., Revuelto, J. & Trigo, R., 2014. Evidence of increasing drought severity caused by temperature rise in southern europe. *Environmental Research Letters,* 9 (4), 044001.

Wei, W.W., 2006. Time series analysis. *The oxford handbook of quantitative methods in psychology: Vol. 2.*

Wilhite, D.A., 2000. Drought as a natural hazard: Concepts and definitions.

Wilhite, D.A. & Glantz, M.H., 1985. Understanding: The drought phenomenon: The role of definitions. *Water international,* 10 (3), 111-120.

Wilson, G.T., 1989. On the use of marginal likelihood in time series model estimation. *Journal of the Royal Statistical Society: Series B (Methodological),* 51 (1), 15-27.

Xie, P., Yatagai, A., Chen, M., Hayasaka, T., Fukushima, Y., Liu, C. & Yang, S., 2007. A gauge-based analysis of daily precipitation over east asia. *Journal of Hydrometeorology,* 8 (3), 607-626.

Yaduvanshi, A., Srivastava, P.K. & Pandey, A., 2015. Integrating trmm and modis satellite with socio-economic vulnerability for monitoring drought risk over a tropical region of india. *Physics and Chemistry of the Earth, Parts A/B/C,* 83, 14-27.

Yurekli, K., Kurunc, A. & Ozturk, F., 2005. Application of linear stochastic models to monthly flow data of kelkit stream. *Ecological modelling,* 183 (1), 67-75.

Zhao, H. & Ma, Y., 2019. Evaluating the drought-monitoring utility of four satellite-based quantitative precipitation estimation products at global scale. *Remote Sensing,* 11 (17), 2010.